Journal of Electrochemistry

Volume 29
Issue 6 *Special Issue on Interfactial Regulation and Electrochemical sensors*

2023-06-28

Metal-Organic Frameworks for Electrochemical and Electrochemiluminescent Immunoassay

Xiao-Li Qin
College of Chemistry and Material Science, Hunan Agricultural University, Changsha 410128, China; Department of Chemistry, Western University, London, ON, N6A 5B7, Canada, qinxl@hunau.edu.cn

Zi-Ying Zhan

Sara Jahanghiri

Kenneth Chu

Cong-Yang Zhang

Zhi-Feng Ding
Department of Chemistry, Western University, London, ON N6A 5B7, Canada, zfding@uwo.ca

Recommended Citation

Xiao-Li Qin, Zi-Ying Zhan, Sara Jahanghiri, Kenneth Chu, Cong-Yang Zhang, Zhi-Feng Ding. Metal-Organic Frameworks for Electrochemical and Electrochemiluminescent Immunoassay[J]. *Journal of Electrochemistry*, 2023 , 29(6): 2218003.
DOI: 10.13208/j.electrochem.2218003
Available at: https://jelectrochem.xmu.edu.cn/journal/vol29/iss6/10

REVIEW

Metal-organic Frameworks for Electrochemical and Electrochemiluminescent Immunoassay

Xiao-Li Qin [a,b,*], Zi-Ying Zhan [b], Sara Jahanghiri [b], Kenneth Chu [b], Cong-Yang Zhang [b], Zhi-Feng Ding [b,*]

[a] College of Chemistry and Material Science, Hunan Agricultural University, Changsha, 410128, China
[b] Department of Chemistry, Western University, London, ON, N6A 5B7, Canada

Abstract

Development of ultrasensitive, highly accurate and selective immunosensors is significant for the early diagnosis, screening, and monitoring of diseases. Electrochemical and electrochemiluminescent (ECL) immunoassays have both attracted great attention and become a current research hotspot due to their advantages such as good stability, high sensitivity and selectivity, wide linear range, and good controllability. Metal-organic frameworks (MOFs), as a new class of porous crystalline materials, have been widely applied in electrochemical and ECL immunosensors owing to their large specific surface area, good chemical stability, as well as adjustable pore size and nanoscale framework structures. Various MOF nanomaterials with different properties for the development of high-performance electrochemical and ECL immunosensors can be achieved, because they can be applied as sensitive platforms for immobilizing biological recognition molecules, enriching the trace analytes and signal molecules, amplifying the signal and enhancing the sensitivity of the electrochemical or ECL immunoassays. This review summarizes various types of MOFs-based immunosensors and their assays application, in which MOFs act as electrode matrices, signal probes (either as electroactive labels or as emitter labels), carriers or catalytic labels for sensitive electrochemical and ECL detections. Moreover, challenges and future opportunities for the development of the functionalized MOFs are discussed to provide a guidance on the design and fabrication of high-performance MOFs-based immunosensors in the future.

Keywords: Metal organic frameworks; Electrochemical immunosensors; Electrochemiluminescent immunosensors; Immunoassays

1. Introduction

Every year, tens of millions deaths occur due to various diseases, such as cancer [1,2], cardiovascular dysfunction (CVD) and chronic respiratory disease (CRD) [3,4]. Early diagnosis has revealed to be an effective route to prevent diseases and enhance survival rates [5,6]. Since clinical studies have proven that biomarker levels correlate well with the severity of the diseases, the sensitive determination of biomarkers is necessary for early diagnosis. Immunosensors, as an important sub-branch of biosensors, employ antibody as a recognition element, which can meet the requirements of specificity and rapidity [7,8]. Conventional immunoassays based on enzyme-linked immunosorbent assay (ELISA) [9,10], chemiluminescence [11,12], fluorescence [13,14], electrochemiluminescence (ECL) [15,16] and electrochemistry [17] have been successfully developed. Among these methods, electrochemical immunoassays have attracted much attention due to their advantages of simple and miniaturized instrumentation, rapid and sensitive detections, and low-costs [18,19]. Furthermore, ECL is also a powerful tool for immunoassay by integrating electrochemical, photoelectrochemoical and

Received 12 November 2022; Received in revised form 2 December 2022; Accepted 7 December 2022
Available online 16 December 2022

* Corresponding author, Xiao-Li Qin, Tel: (86-731) 84617022, E-mail address: qinxl@hunau.edu.cn.
* Corresponding author, Zhi-Feng Ding, Tel: (519) 661-2111 ext. 86161, E-mail address: zfding@uwo.ca.

https://doi.org/10.13208/j.electrochem.2218003

spectroscopic techniques, which involves the electron-transfer reactions of electro-generated species to form excited states that emit light [16]. To improve performances and increase functions of immunosensors, many studies have mainly focused on signal amplification and noise reduction because of the weak electrochemical activities of antigen and antibody [20]. To date, various materials have been introduced to amplify the electrochemical signals and obtain the high sensitivity, such as enzyme [9], nanomaterials [21], highly branched polymers [22] and traditional redox compounds [18]. Nanomaterials have been proven to be outstanding because of their small size effects, and unique optical, electrical, magnetic, mechanical and catalytic properties. As "the most promising materials" of the 21st century, nanomaterials not only can be used as the signal amplification labels on electrochemical immunosensors, but also as a modifier of electrodes to create nanostructure surfaces with fast electron transfer and low background current.

To effectively amplify sensitivity, all kinds of nanomaterials have been applied in electrochemical immunoassays, including carbon nanomaterials [23], semiconductor quantum dots [24], noble metal nanoparticles [25,26] and porous materials [27]. In particular, metal-organic frameworks (MOFs) [28], as a new class of crystalline porous materials, possess advantages over other nanomaterials including their good biocompatibility, excellent catalytic activity and tunable structure, composition and pore size, which show fascinating physical/chemical properties and widespread applications [29], especially in electrochemical immunosensing [17]. For example, the merits of good biocompatibility and large surface area of MOFs make them easy to conjugate or load multifarious biomolecules (i.e., antigen, antibody or enzyme), nanoparticles and electroactive tags [30]. Moreover, some conductive MOFs or MOF composites can promote electron transfer between biological elements and electrode surfaces [31]. Most importantly, MOFs with tunable structure, high porosity, and controllable hydrophilic and hydrophobic pore nature exhibit highly efficient catalysis under mild conditions, which offer a new window for electrochemical immunoassays [32]. Indeed, MOFs have been widely used in immunoassay and made unbelievable progress in the past decade, promoting the development of immunoassays.

Until now, numerous excellent reviews that focus on the synthesis methods and functional applications of MOFs, such as catalysis, energy, gas storage and separation, electron and optoelectronic devices, drug/cargo delivery and cancer therapy, have been published [33]. In recent years, the rise in the popularity of MOFs-based composites has led to numerous papers utilizing the MOFs-based materials for electrochemical applications [34,35]. Thus, this review will highlight the development of electrochemical immunoassays based on MOFs over the past few years, including individual and multifunctional immunosensing platforms. In addition, research in the fields of ECL immunoassays with MOFs is also summarized. Finally, this review provides an outlook for the development of electrochemical and ECL immunosensing MOF platforms, and their potential clinical applications.

2. MOFs for electrochemical immunoassay

2.1. MOFs as matrices for label-free electrochemical sensing

Electrode materials are vital for fabricating electrochemical immunosensors, because they are not only responsible for improving the electronic transmission rate to enhance the electrochemical signal, but also for increasing specific electrode surface area to immobilize more antibodies or electroactive molecules [20]. MOFs-based compounds have been proven as promising electrode materials for anchoring various biomolecules or probes [36]. For example, on the base of SiO_2@UiO-66 nanocomposite, Mehmandoust's group [37] developed a label-free electrochemical immunoassay for rapid and selective detection of SARS-CoV-2 spike protein (SARS-CoV-2 S-protein) by electrochemical impedance spectroscopy (EIS) (Fig. 1), which showed a range of 100.0 fg·mL^{-1} to 10.0 ng·mL^{-1} with a detection limit (LOD) of 100.0 fg·mL^{-1}. This as-prepared sensor can directly analyze the electrochemical interactions between the viral protein and electrode-electrolyte interface of the sensor. Li et al. [38] utilized $ZrOCl_2$ as a metal precursor and 5,10,15,20-tetra(4-aminophenyl) porphyrin as an organic ligand to prepare a Zr-TAPP MOF nanocarrier for label-free impedimetric immunoassay of neuron-specific enolase (NSE). The Zr-TAPP MOFs presented strong affinity to the NSE antibody due to the amino groups, Zr(III) coordination centers and π-π* bonds, resulting in a wide linear range of 10.0 fg·mL^{-1} to 2.0 ng·mL^{-1} and a low LOD of 7.1 fg·mL^{-1} for sensitive NSE determination.

As proven in previous reports, the isostructural bimetallic MOFs exhibited good stability and excellent biocompatibility for various biosensors [39]. For example, Song et al. [40] reported an impedimetric immunosensor based on a bimetallic CoNi-MOFs for sensitive detections of deoxynivalenol (DON) and salbutamol (SAL), measuring

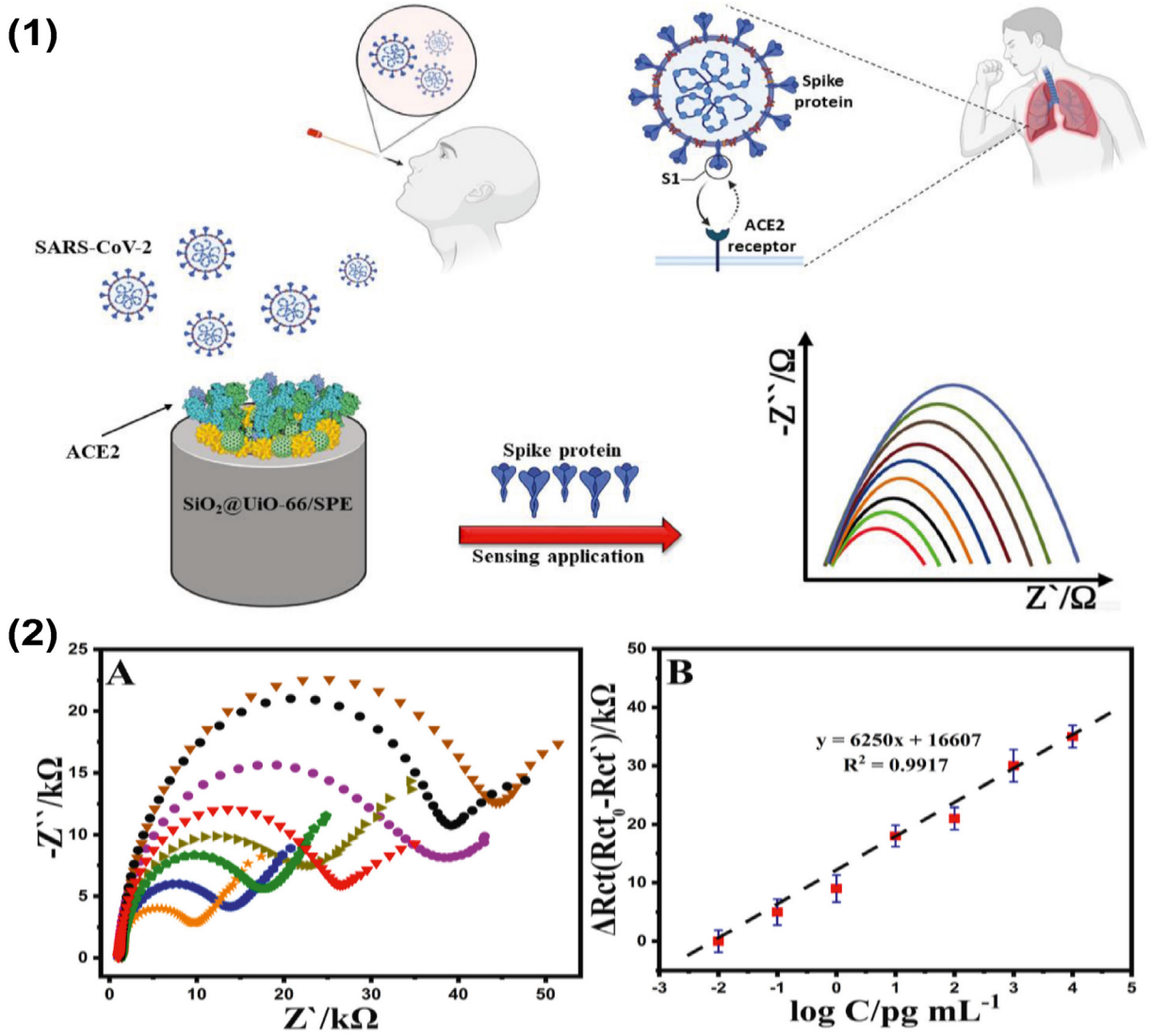

Fig. 1. (1) Schematic of the preparation and act mechanism of immunosensor. (2) Nyquist plots obtained with SiO_2@UiO-66/SPCE at various concentrations of SARS-CoV-2 protein S-protein (A) and the plot of logarithm concentrations against ΔR_{ct} (B). Reproduced with permission of Ref. [37], copyright 2022 Elsevier B.V.

by EIS in $[Fe(CN)_6]^{3-/4-}$ solution to evaluate the performance of immunosensor. The values of charge transfer resistance (R_{ct}) obtained from the Nyquist plots of immunosensor gradually increase along with increasing the DON/SAL concentrations, which is a consequence of the efficient immune recognition of DON/SAL by immunosensor, via the increased formation of Ab_{DON}-DON/Ab_{SAL}-SAL complex at the modified electrode surface. Thus, the variation of R_{ct} values (ΔR_{ct}) for the developed immunosensor before and after DON/SAL detections is proportional to the logarithm value of the DON/SAL concentration. The CoNi-MOFs with a small particle size and a good electrochemical activity were synthesized by using the mixed organic linkers of 4-(1H-tetrazol-5-yl) benzoic acid (H_2TZB) and 2,4,6-tri(4-pyridyl)-1,3,5-triazine (TPT), presenting an excellent bioaffinity toward analytes due to the π-π* stacking, and the electrostatic interaction between the carboxyl groups of CoNi-MOF and the amino groups of antibodies. Thus, this electrochemical immunosensor realized the high immobilization amounts of antibodies and high sensitivity with low detection limits of 0.05 and 0.30 $pg \cdot mL^{-1}$ toward, respectively, DON and SAL in the concentration range of 0.001−0.5 $ng \cdot mL^{-1}$.

Metal nanoparticles with excellent catalytic property and unique structure, can be combined with MOFs as a good electrode substance for the enhancement of electrochemical signals and the immobilization of biomolecules [41]. For example, Tang and co-workers [17] used the platinum nanoparticles (PtNPs) and 2D Zn-Hemin MOF

composites to conduct a label-free electrochemical immunosensing platform for sensitive detections of pig immunoglobulin G (IgG) and surface-protective antigen (Spa) protein of *Erysipelothrix rhusiopathiae*. The PtNPs/Hemin-MOFs modified on the electrode surface not only served as the peroxidase mimics to catalyze the H_2O_2 due to the existence of iron active sites in hemin and PtNPs, but also acted as an anchor to capture the antibody. The electrochemical signal from the immunoelectrode gradually weakened with increasing the concentration of antigen, because more specific binding sites of antigen decreased in the specific recognition progress. Thus, the as-prepared electrochemical immunosensor for IgG and Spa detections is in wide ranges with low LODs. Cao's group [42] reported an electrochemical immunosensor based on AuNPs@ZIF-8 and multiwalled carbon nanotubes (MWCNTs) nanocomposites as support for detecting the alpha fetoprotein (AFP) in serum. The AuNPs@ZIF-8@MWCNTs with excellent electrical conductivity acted as an ideal nanocarrier to increase target molecular loading due to their large surface area and abundant binding sites, which can enhance electrochemical signals for sensitive AFP detection in the range of 0.1 $pg\cdot mL^{-1}$ to 100 $ng\cdot mL^{-1}$ with a low LOD of 0.033 $pg\cdot mL^{-1}$.

2.2. MOFs as labels for sandwich-type electrochemical sensing

2.2.1. MOFs used as electroactive labels

MOFs can be directly used as electroactive labels to amplify the electrochemical signal in a sandwich-type immunosensor. MOFs can be specifically coupled to the surface of modified electrode after immunoreaction. Generally, to monitor the target concentrations, some acidic solutions are utilized to dissolve the MOFs to metallic ions (e.g., Cu^{2+} and Ag^{+}), and then these dissolved ions are sensitively detected by the anodic stripping voltammetry (ASV). As shown in Fig. 2, Xie's group [43] employed the carboxyl groups of HKUST-1 to immobilize the secondary antibody of NT-proBNP for biolabeling, and the Cu^{2+} in the HKUST-1 biolabel was detected by linear sweep ASV (LSASV) in 0.1 $mol\cdot L^{-1}$ HNO_3 + 1 $mol\cdot L^{-1}$ NaCl directly on the immunoelectrode. Then, the oxidation peak current of Cu increased gradually with the increase of NT-proBNP protein concentration from 0.5 $fg\cdot mL^{-1}$ to 500 $ng\cdot mL^{-1}$, and the LOD was 0.33 $fg\cdot mL^{-1}$ ($S/N = 3$). Some other examples are listed in Table 1.

2.2.2. MOFs used as electrocatalytic labels

Recently, various MOFs have been employed as efficient electrocatalytic labels in electrochemical immunoassays for enhancing the detection of biomolecules, which are more convenient and lower cost than that of the enzyme-involving amplified assay strategies.

A series of MOFs, such as based on iron and copper, can effectively trigger the reaction rate of Fenton-like reaction [18]. For example, Liu et al. [47] fabricated an electrochemical immunosensor using $Cu_3(BTC)_2$ (BTC = benzene-1,3,5-tricarboxylic acid) MOF as nonenzymatic label conjugated secondary antibody for sensitive detection of prostate specific antigen (PSA). The highly electrocatalytic activity of the $Cu_3(BTC)_2$ MOF toward H_2O_2 provides amplified sensitivity of immunosensor, achieving a wide linear range from 0.1 to 10 $ng\cdot mL^{-1}$ with LOD of 0.025 $ng\cdot mL^{-1}$ for the detection of PSA, which is attributed to its catalytic and coordination sites on the Cu(II) centers. Due to the existence of copper active sites, the Cu-MOFs conjugated with glucose oxidase (GOx) and antibody were used to develop a cascade catalysis-initiated radical polymerization with impedimetric immunosensor for detection of carbohydrate antigen 15-3 (CA15-3) (Fig. 3) [48]. When GOx catalyzed the oxidation of glucose to generate H_2O_2, Cu-MOFs subsequently catalyzed the H_2O_2 to react with acetylacetone (ACAC) and yielded ACAC radicals for the in-situ formation of poly(N-isopropylacrylamide) (PNIPAM) with poor conductivity on the substrate, which can hinder the charge transfer of $[Fe(CN)_6]^{3-/4-}$ and elevate the resistance difference. This designed immunosensor for CA15-3 displayed wide detection ranges of 10 $\mu U\cdot mL^{-1}$ − 10 $mU\cdot mL^{-1}$ and 10 $mU\cdot mL^{-1}$ − 100 $U\cdot mL^{-1}$ with low LOD of 5.06 $\mu U\cdot mL^{-1}$.

In order to improve the catalysis of H_2O_2, some multifunctional Fe-MOFs immunoprobes were fabricated with metal nanocomposites, such as AuNPs [49], MoS_2 [50], which holds great promise for sensitive signal amplification in electrochemical immunoassays. Besides these, Zhang et al. [51] developed an electrochemical immunosensor for microcystin-LR detection by AuNPs@MIL-101 (Cr(III)-MOFs) immunoprobes, which owns strong catalytic properties to the oxidation of ascorbic acid (AA). This competitive microcystin-LR immunosensor showed a linear range of 0.05 $ng\cdot mL^{-1}$–75 $\mu g\cdot mL^{-1}$ with LOD of 0.02 $ng\cdot mL^{-1}$.

2.2.3. MOFs used as carriers

With the high porosity, good stability, large specific area and surface easy functionalization, MOFs have become ideal carriers to load various biomolecules, multipurpose nanocomposites, and multiple of electroactive labels for enhancing the signal response of the electrochemical immunosensors [52]. These biomolecules and nanocomposites not only can be modified in the cavity

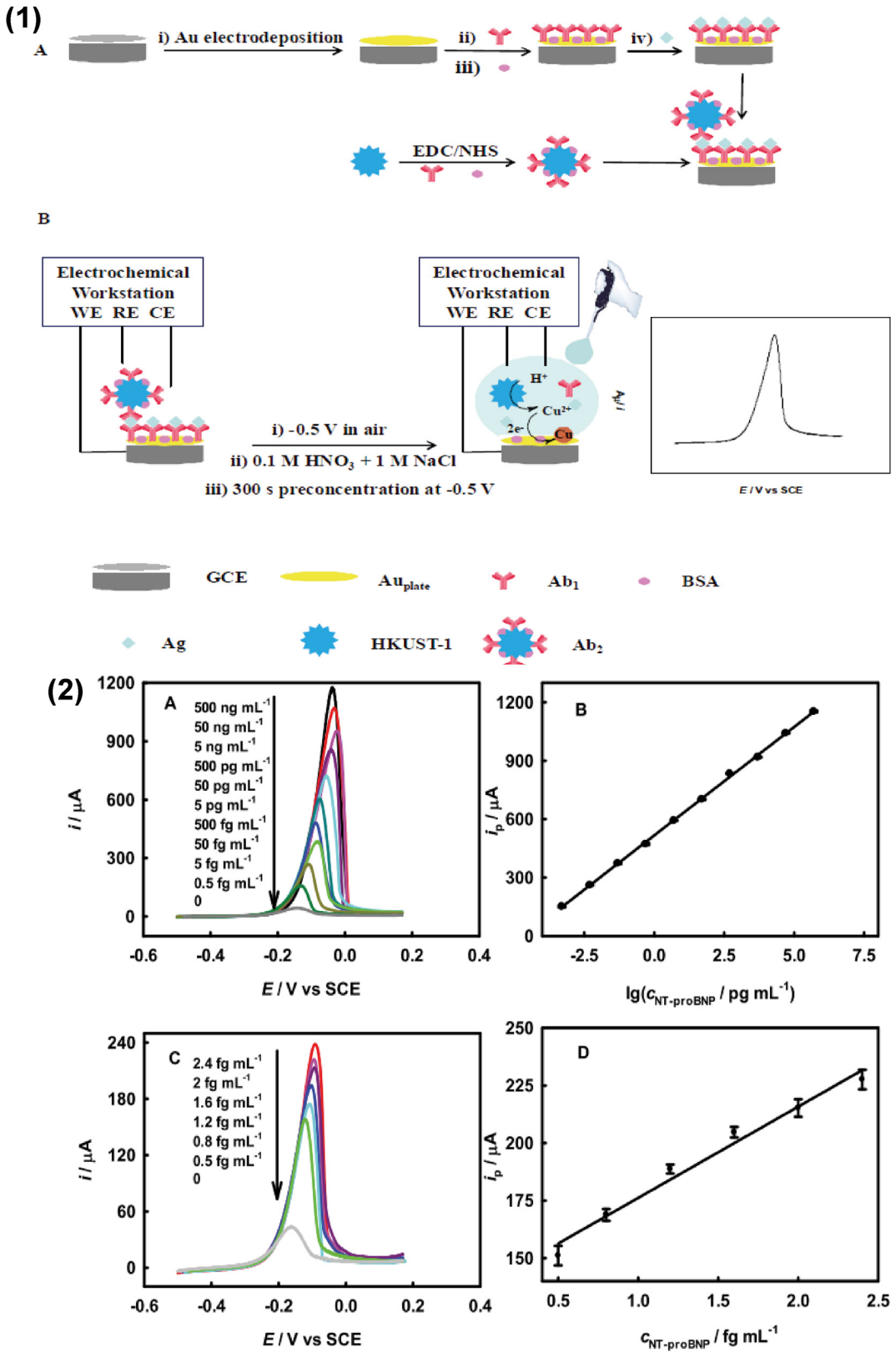

Fig. 2. (1) Illustration of the MOFs-based immunoelectrode preparation. (2) LSASV curves for high-concentration (A) and low-concentration (C) NT-proBNP immunoassay using our method and the corresponding calibration curves (B and D) (n = 3). Scan rate: 100 mV·s^{-1}. Reproduced with permission of Ref. [43], copyright 2020 Wiley-VCH.

Table 1. MOFs as electroactive labels for electrochemical immunoassays.

Sensor material	Target	Linear range ($ng \cdot mL^{-1}$)	LOD ($ng \cdot mL^{-1}$)	Ref.
HKUST-1 Cu-MOFs	NT-proBNP	0.5×10^{-6}–500	0.33×10^{-6}	[43]
Ag-MOFs	CEA	0.05–120	8×10^{-6}	[44]
AuNPs/Cu-MOFs	C-reactive protein	1–400	0.2	[45]
AuNPs/Cu-MOFs	CEA	0.1–80	0.03	[46]

NT-proBNP: amino-terminal pro-B-type natriuretic peptide; CEA: carcinoembryonic antigen.

of MOF, but also can be connected on the surface of MOF. Besides that, the electroactive molecules, such as organic carboxylates and multi-nitrogen compounds, also can act as the organic linkers in MOFs by oxygen- or nitrogen-coordination.

Frequently, these immobilized biomolecules are the antibody and enzyme molecules [53]. For example, Ma's group [54] employed ZIF-8 as a carrier to absorb thionine and bovine serum albumin (BSA), which acted as an anchor to attach the labeling secondary antibody (Ab_2) and alkaline phosphatase (ALP) to improve the detection performance of the electrochemical immunosensor for carbohydrate antigen 72-4 (CA 72-4) (Fig. 4). Because, in the presence of CA72-4 on a sandwich immunosensor, a cascade reaction chain was introduced to deposit silver nanoparticles (AgNPs) under the catalysis, improving the conductivity of electrode interface. Thus, this immunosensor presented good performance with a linear range from 1.00 $\mu U \cdot mL^{-1}$ to 10.0 $U \cdot mL^{-1}$ and a LOD of 0.438 $\mu U \cdot mL^{-1}$ ($S/N = 3$). On the base of i-motif DNA structure modified UiO-66-NH_2, Feng et al. [55] designed an electrochemical immunosensor of squamous cell carcinoma antigen (SCCA) through a proton-activated annunciator for responsive release of methylene blue (MB). A ZIF-8 immunoprobe contained GOx was used to catalyze the glucose and then produced the protons, which acted as the key to unlock the i-motif functionalized UiO-66-NH_2 and released the loaded MB electroactive molecules, improving the electrochemical response. Under the optimal conditions, this immunosensor displayed good performance with a linear range from 1 $\mu g \cdot mL^{-1}$ to 1 $pg \cdot mL^{-1}$ and a LOD of 1.504 $fg \cdot mL^{-1}$ ($S/N = 3$). As mentioned above, MOFs can be modified with biomolecules to prepare labels and construct electrochemical immunosensors. Nevertheless, the signal amplification ability is limited.

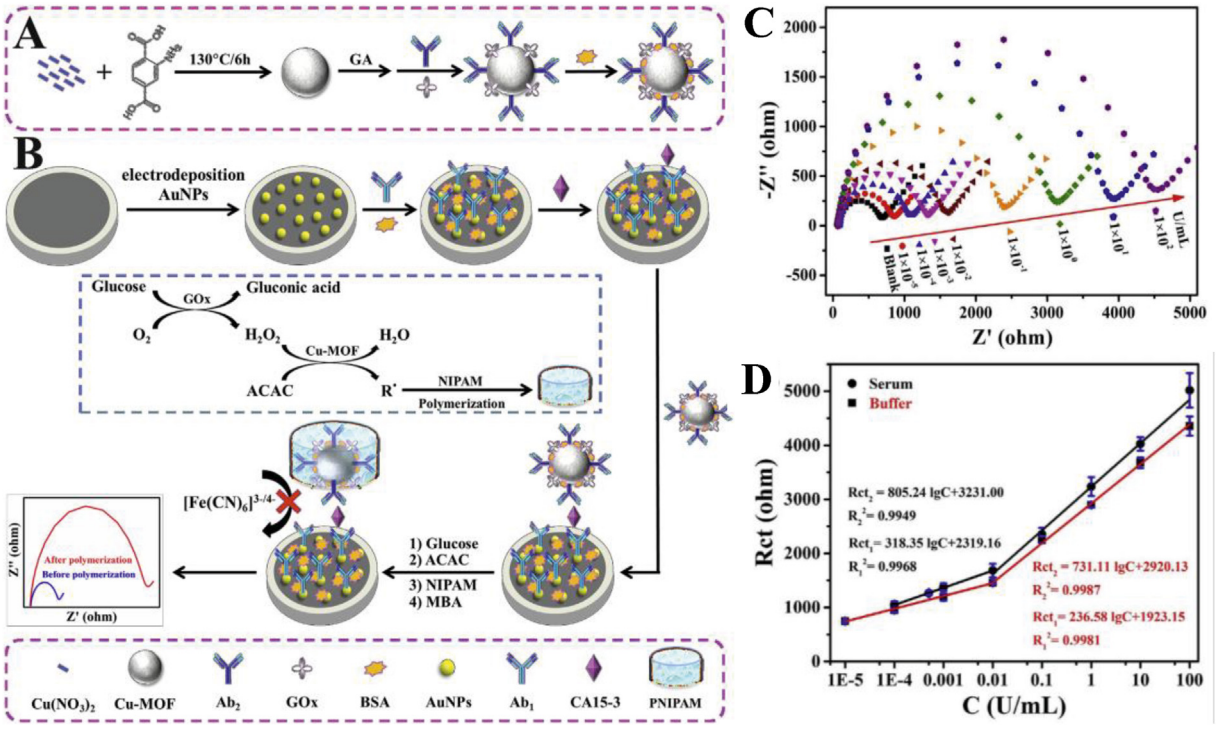

Fig. 3. Schematic illustrations of preparation process of immunoprobes (A) and cascade catalysis-initiated radical polymerization triggered signal amplification for electrochemical detection of CA15-3 (B). (C) EIS responses of electrochemical biosensor for target CA15-3 from blank to 100 $U \cdot mL^{-1}$ in buffer solution. (D) The calibration curves of resistance values vs. the concentrations of CA15-3 in buffer solution (■) and human serum (●). Reproduced with permission of Ref. [48], copyright 2019 Elsevier B.V.

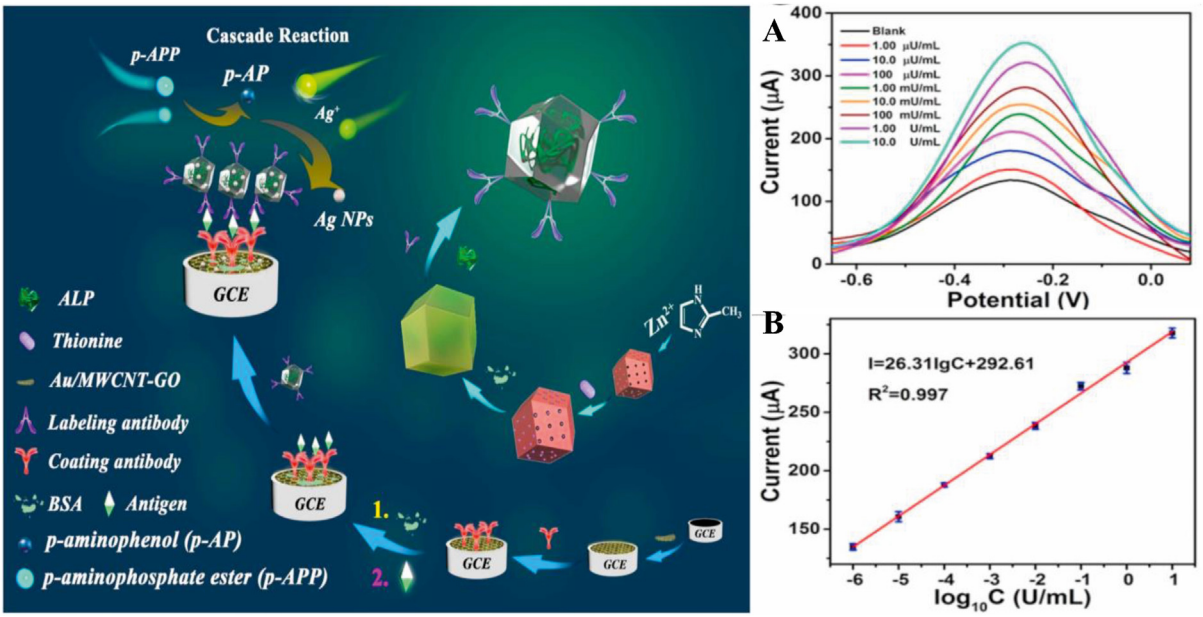

Fig. 4. Construction steps and mechanism of immunosensor (left). (right) SWV responsess of immunoassay for CA 72-4 in 1 mmol·L^{-1} PBS (pH 7.5) at concentrations from 1.00 μU·mL^{-1} to 10.0 U·mL^{-1} (A); Calibration plot (B) between SWV peak current (0.18 V vs. Ag/AgCl) and logarithm values of CA 72-4 concentrations (the error bars are standard deviations for n = 3). Reproduced with permission of Ref. [54], copyright 2021 Elsevier B.V.

The rapidly emerging research field of metal nanocomposites provides great possibilities to advance development of signal amplification strategies for sensitive electrochemical detection [21]. Generally, MOFs are combined with metal nanocomposites to improve the biocompatibility, catalytic ability and electrical conductivity. Li and co-workers [56] used hyaluronic acid (HA) modified Ce-MOFs as the skeleton precursor, loading with AgNPs and horseradish peroxidase (HRP) to catalyze H_2O_2, which can double amplify the electrochemical signal (Fig. 5 (left)). This immunosensor for CEA detection displayed a broad linear response range between 1 pg·mL^{-1} and 80 ng·mL^{-1}, and the LOD was at 0.2 pg·mL^{-1}. Qin's group [32] reported a sensitive electrochemical immunosensor for foot-and-mouth disease virus (FMDV) based on a simple strategy of in-situ selective growth CdS nanocystalline on Zn-MOFs (Fig. 5 (right)). With increasing the target concentration, more Zn-MOFs-Ab_2 was fixed on the surface of immunosensor and then more CdS was deposited catalytically on the Zn-MOFs surface, which can increase the current intensity. Therefore, the immunoassay of FMDV showed a good linear response range from 0.5 fg·mL^{-1} to 5 ng·mL^{-1} with a LOD of 0.05 fg·mL^{-1} (see Fig. 6).

The electroactive molecules, such as ferrocene (Fc) and toluidine blue (TB), are the most commonly used electroactive labels, which usually combine with MOFs through electrostatic interaction and covalent linkage, directly producing electrochemical signals. Han et al. [57] employed Fc confined in Zn-MOF (Fc-Zn-MOF) as an electrochemical signal tag to fabricate an immunosensor for sensitive amyloid-β (Aβ) detection, with a linear ranging from 0.1 pg·mL^{-1} to 100 ng·mL^{-1} and a detection limit of 0.03 pg·mL^{-1}. Liu and co-workers [58] fabricated a sandwich immunosensor for sensitive detection of CEA by using TB loaded Cu-MOFs with polydopamine (PDA) coating (Cu-MOFs-TB/PDA) as a signal probe, and chitosan and MWCNTs on the glassy carbon electrode (GCE) to immobilize antibody. HCl was used to destroy the immune complex and probe, resulting in the increased response current because of the closer distance between TB and the electrode. Thus, CEA was detected with a linear range from 20 fg·mL^{-1} to 200 ng·mL^{-1} and a LOD of 3 fg·mL^{-1} ($S/N = 3$). Lu's group [59] employed Nile Blue, as a kind of redox-active species, decorated ZnNi-MOF (NB@ZnNi-MOF) spheres immobilized with human chorionic gonadotropin (HCG) Ab_2 for signal amplification, consequently fabricated a three-dimensional CoNi-MOF nanosheet array-based immunosensor for sensitive monitoring of HCG with core-shell NB@ZnNi-MOF nanotags. This HCG immunosensor displayed a wide linear range from 0.005 mlU·mL^{-1} to 250 mlU·mL^{-1} and a low LOD (1.85×10^{-3} mlU·mL^{-1}) detection.

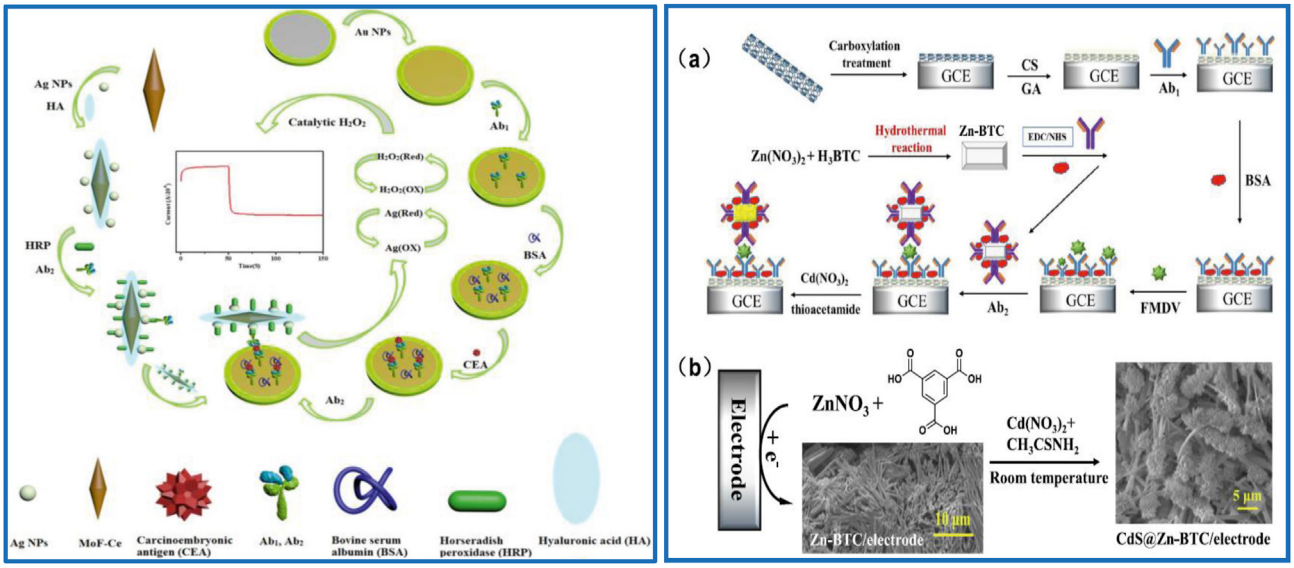

Fig. 5. (left) A schematic of sensitive detection of CEA by a sandwich-type electrochemical immunosensor using MOF-Ce@HA/Ag-HRP-Ab_2 as a nanoprobe. Reproduced with permission of Ref. [56], copyright 2020 IOP Publishing. (right) A schematic diagram of immunosensor construction (a) and preparation of CdS@Zn-BTC modified electrode (b). Reproduced with permission of Ref. [32], copyright 2021 Elsevier B.V.

2.3. MOFs as labels for simultaneous electrochemical immunoassays of multiple biomarkers

The simultaneous determination of multiple biomarkers plays an important role in early diagnosis and screening of disease. Zhang et al. [60] designed a strategy for the simultaneous determination of CEA and AFP by using two aminated MOFs prepared from Pb(II) or Cd(II) and 2-aminoterephthalic acid to label the Ab_2 for signal amplification. In a sandwich immunoassay, these two MOFs labels were dissolved by acid (HNO_3) and then the contents of Pb^{2+} and Cd^{2+} were determined simultaneously to qualify CEA and AFP, respectively, in an ASV method. This assay has a linear range from 0.3 pg·mL^{-1} to 3 ng·mL^{-1} of both CEA and AFP, and the LODs are 0.03 pg·mL^{-1} and 0.1 pg·mL^{-1}, respectively, which may be widely applied to the simultaneous detection of multiple biomarkers in the future.

3. MOFs for ECL immunoassays

Although the high performance and the related analytical method of electrochemical immunosensors are expected to find wide applications in the detection of various biomarkers in complex biological samples, the sensitivity is not as good as an ECL immunosensor. ECL immunosensing platform has attracted much attention in analytical methods because of its low background signal, ease of operation, high sensitivity and fast response. In particular, MOFs coupled with ECL measurement have been focused on the various analyte detections.

3.1. MOFs as an emitter for ECL immunoassay

The successful use of ECL immunoassay in clinical diagnosis requires development of novel ECL signal probes. Thus, some MOFs as ECL signal emitters in the ECL immunoassay have been reported [61]. For example, Wang et al. [62] prepared self-luminescent lanthanide (Ln)-MOFs (LMOFs) from precursors containing Eu(III) ions and 5-boronoisophthalic acid (5-bop) to adjust optical properties and investigate the ECL emission mechanisms. Combined with the NiFe composites as a carrier, this LMOF as a signal probe exhibited excellent performance characteristics in an ECL immunoassay of Cytokeratins21-1 (cyfra21-1) with a LOD of 0.126 pg·mL^{-1} (Fig. 7), which has great significance in the diagnoses of lung cancer, breast cancer and lung or esophageal squamous cell carcinoma. Ju's group [63] reported a signal amplification strategy for ECL immunoassay by employing Cu-doped terbium luminescent MOFs (Cu:Tb-MOFs) as an emitter and a coreaction promoter. On the base of the low electron transfer resistance of Cu:Tb-MOFs, a label-free ECL pro-gastrin-releasing peptide (ProGRP, a biomarker of small-cell lung cancer) immunosensor displayed good performance with a detection range between 1.0 pg·mL^{-1} and 50 ng·mL^{-1} with a LOD down to 0.68 pg·mL^{-1} (3σ). Besides, Song et al. [64] employed 3,4,9,10-perylenetetracarboxylic (PTC) as ligands to develop a Zn-PTC MOF as an effective ECL probe for trace detection of trenbolone (TBE). This Zn-PTC with the metal-to-ligand charge-transfer (MLCT) effect could

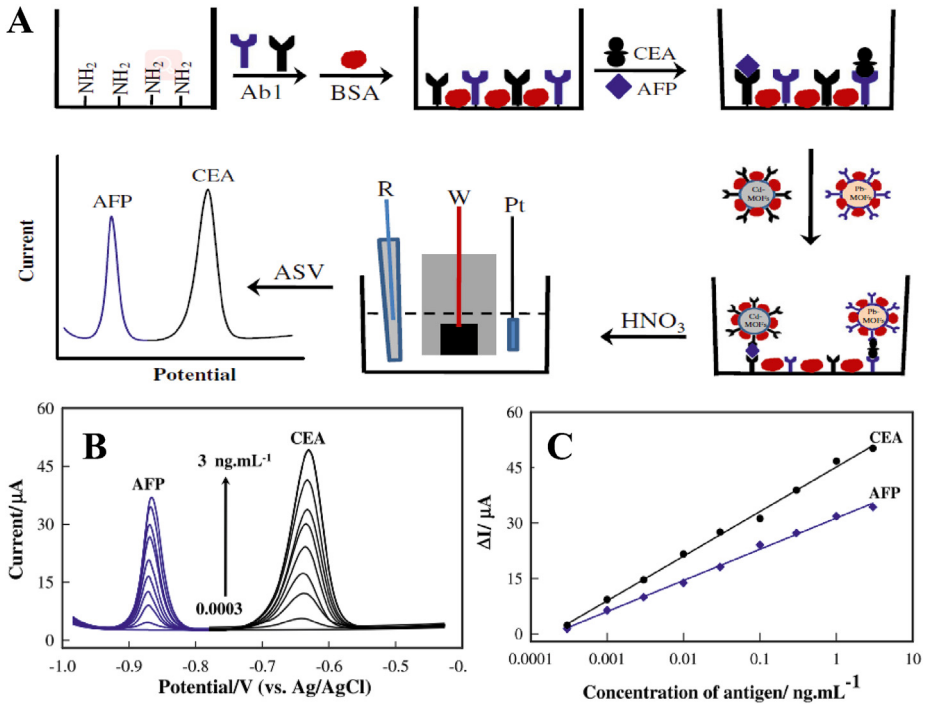

Fig. 6. (A) Schematic illustration of the stepwise immunoanalysis process. (B) Typical DPASV curves of the immunosensors for different AFP and CEA concentrations. (C) The resulting calibration curves of antigens plotted on a semilog scale. Reproduced with permission of Ref. [60], copyright 2017 Springer-Verlag GmbH Austria.

achieve the energy transfer from Zn^{2+} to the ligand for strong luminescence. Therefore, the constructed competitive immunosensor realized trance detection of TBE with a detection range from 10 fg·mL^{-1} to 100 ng·mL^{-1} and a low LOD of 3.28 fg·mL^{-1}.

The embedding of *in situ* coreactant into ECL protocol can obviously enhance the ECL signal, and improve the detection sensitivity. Wei's group [65] constructed a dumbbell plate-shaped Zr-TCBPE MOF as ECL tags with high luminous efficiency by combining the 1,1,2,2-tetra(4-carboxylbiphenyl)ethylene (H_4TCBPE) with Zr(IV) cations. Then, the uniquely self-enhanced ECL complex of Zr-TCBPE-PEI was formed by covalently connecting polyethyleneimine (PEI) as the coreactant with MOF, which presented the robust ECL signal thanks to the intramolecular-like coreaction acceleration. A sandwich-type ECL immunosensor was constructed for sensitive detection of neuron-specific enolase (NSE) with a LOD down to 52 fg·mL^{-1}.

3.2. MOFs as a carrier for ECL immunoassay

At present, most of the reported methods have used MOFs as carriers to immobilize the typical ECL emitters or coreactants due to their ultrahigh surface area, high poriness and easy functionalization. For example, Yang et al. [66] constructed a sensitive immunosensor by using an isoreticular MOF (IRMOF-3) accelerator enriched a large amount of CdTe QDs (CdTe@IRMOF-3@CdTe) as a signal probe for the detection of trace cardiac troponin-I antigen (cTnI) (Fig. 8). This coreactant accelerates for promoting the conversion of coreactant $S_2O_8^{2-}$ into the sulfate radical anion ($SO_4^{\bullet-}$), which can boost the ECL emission of CdTe. Thus, the immunosensor using CdTe@IRMOF-3@CdTe labeled antibody as the signal probe displayed good performance for cTnI with a wide linear range from 1.1 fg·mL^{-1} to 11 ng·mL^{-1} and a low LOD of 0.46 fg·mL^{-1}.

Among numerous illuminants, $Ru(bpy)_3^{2+}$ is a prevalent luminophore, which can be intergrated into the pores of the MOF structure and strongly absorbed on the surface of nanoparticles. Zhao et al. [79] fabricated a sensitive sandwich-type immunosensor for insulin detection, on the base of the resonance energy transfer (RET) between UiO-67/$Ru(bpy)_3^{2+}$ (ECL donor) and Au@SiO_2 nanoparticles (ECL acceptor), resulting in a decreased ECL response. The ECL decrease efficiency was related to the concentration of insulin antigen in the range from 0.0025 to 50 ng·mL^{-1} with a LOD of 0.001 ng·mL^{-1}.

Coreactants for ECL system are also the key in the coreactant-involved approach. Thus, Shao's group [80] developed a strategy for *in situ* growth

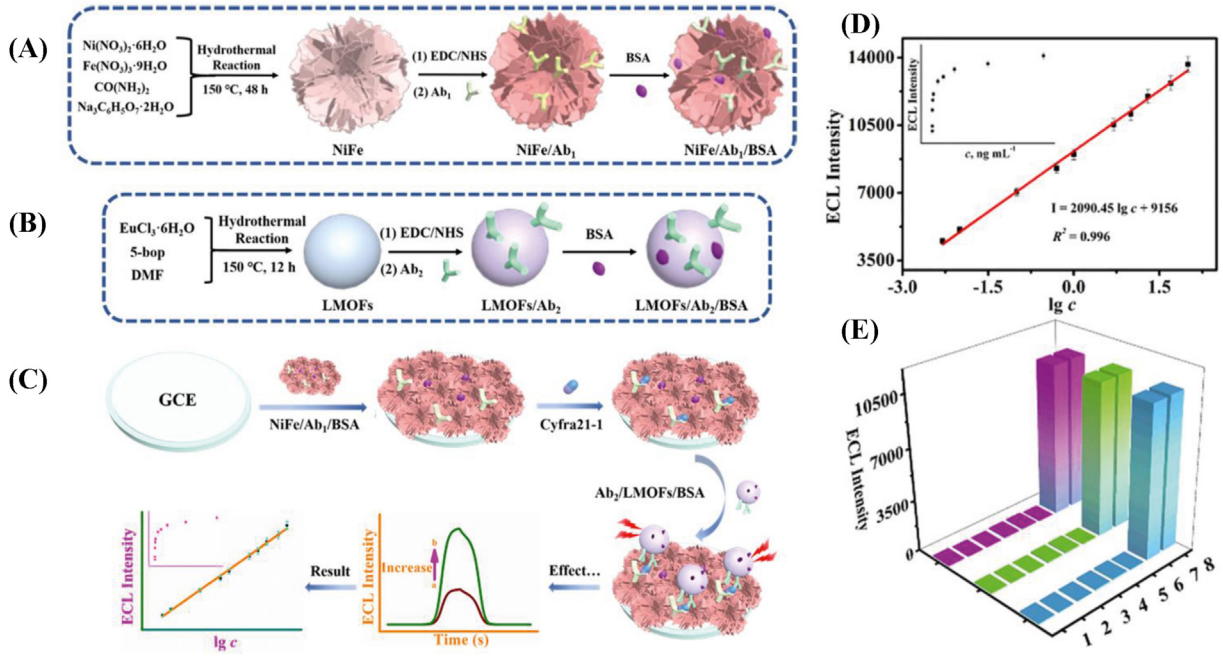

Fig. 7. Preparation of NiFe complex/Ab_1/BSA bioconjugate (A), Ab_2/LMOFs/BSA bioconjugate (B), and formation route of the suggested signal-enhanced ECL model (C). Working curve (D) of the signal-enhanced ECL detection model for different concentrations of cyfra21-1 (0.00500, 0.0100, 0.100, 0.500, 1.00, 5.00, 10.0, 20.0, 50.0, and 100 ng·mL^{-1}). Selectivity (contents of cyfra21-1 and other interferents were 10.0 and 100 ng·mL^{-1}, respectively. Error bars = SD (n = 3). (E) Plots of the ECL detection model. Reproduced with permission of Ref. [62], copyright 2021 American Chemical Society.

of the triethanolamine (TEOA)-functionalized MOFs (TEOA@MOFs) on the GO nanosheets, in which both TEOA and GO can act as the coreactant for $Ru(bpy)_3^{2+}$ ECL system. Then, a label-free ECL immunosensor based on the GO-TEOA@MOFs nanocomposites modified electrode was conducted for sensitive determination of human copeptin, and the linear range was from 5 pg·mL^{-1} to 500 ng·mL^{-1} with a LOD of 360 fg·mL^{-1}. The research on this protocol is not as intense as that on electrochemical methods. However, ECL immunoassays generally exhibit higher detection sensitivity than electrochemical ones. As shown in Table 2, these representative examples proved that femtogram ultrasensitive detection of low-level analytes were achieved by MOFs-based ECL immunoassays.

4. Conclusions and future prospects

MOFs, an attractive class of crystalline porous materials, have enriched the diversity of designing electrochemical and ECL immunosensors, which are of great importance to immunoassays and have attracted much attention from the academic communities. Various works above, prove the broadness of bio-functionalized MOF nanocomposites for the amplification of the electrochemical and ECL signals of immune recognition events, which can remarkably change the electrochemical or ECL signal related to the content of biomarkers. To date, different designs and fabrication strategies for the development of MOF-based electrochemical and ECL immunosensors are described as the following. As an emitter or electroactive labels connected with antibody to obtain electrochemical or ECL signal.

1) As carriers for the biomolecules (e.g., antibody and enzyme), nanoparticles (e.g., AuNPs and AgNPs), and electroactive/ECL probes and signal molecules (e.g., metal ions, luminescent and electroactive molecules). As indicators to induce the deposition of CdS nanolabels.

2) As efficient catalytic labels for catalytic events, such as the catalytic reductions of H_2O_2, oxygen and AA.

Nevertheless, there are still some challenges in order to obtain more highly effective MOF-based immunosensors. Firstly, the poor conductivity of these MOFs is always a limitation to restrict the electron transfer when they are modified on the surface of electrodes, resulting in the decreasing of electrochemical or ECL signals. To obtain a great sensitive and accurate immunosensor, conductive MOFs can be applied to promote the mass/electron transport efficiency. Secondly, the applications of MOFs in sensing, therapeutic or imaging are greatly hindered due to the lack of water-stable MOFs with sufficient catalytic activity. To achieve high performance in these applications, exploring

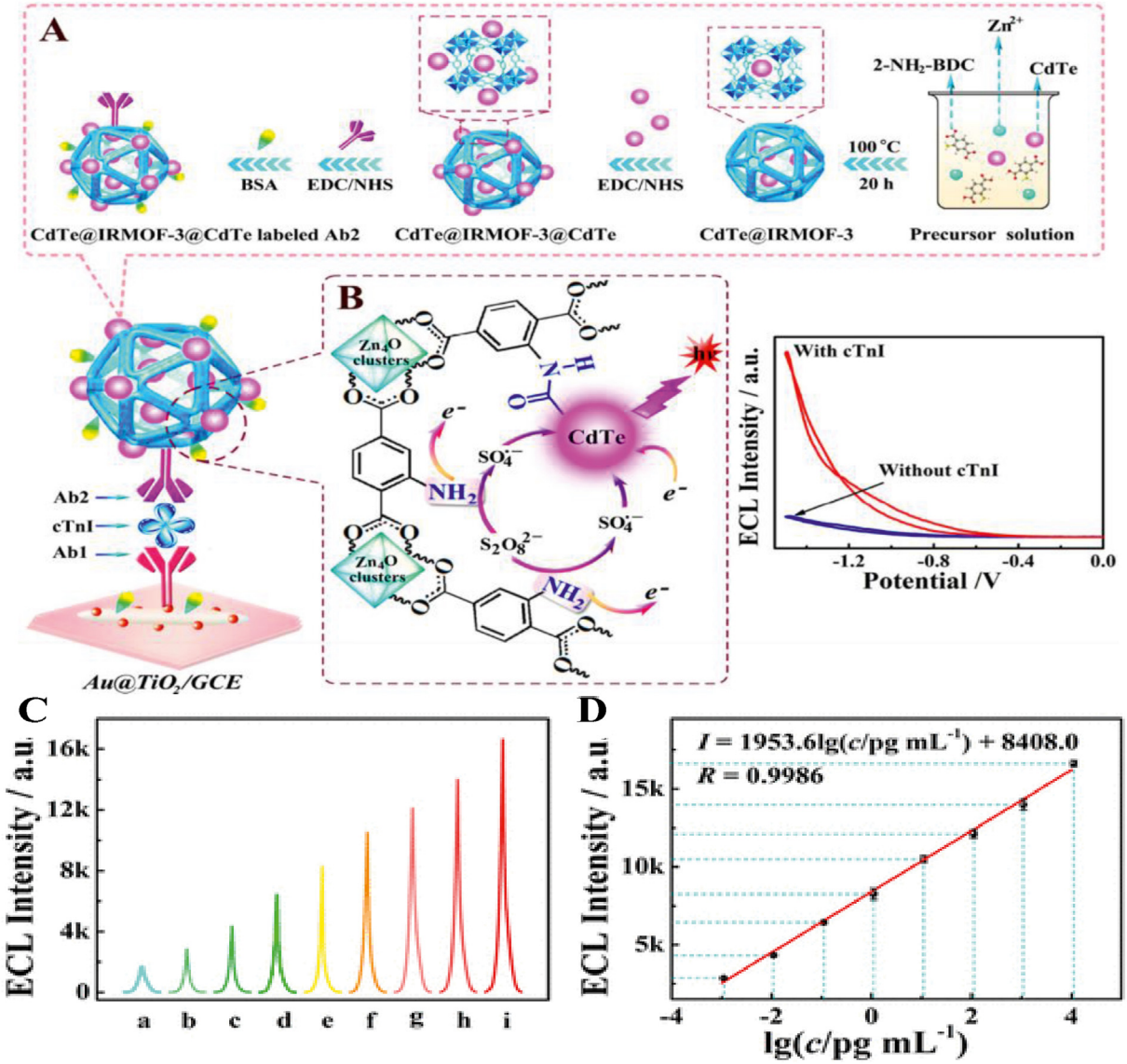

Fig. 8. (A) Preparation of the CdTe@IRMOF-3@CdTe labeled signal probe. (B) Possible mechanism of IRMOF-3 accelerator-mediated enhancement of cTnI detection in the CdTe/$S_2O_8^{2-}$ system. (C) ECL intensity-time plots of the proposed immunosensor incubated with cTnI at different concentrations: (a) 0, (b) 1.1 fg·mL^{-1}, (c) 11 fg·mL^{-1}, (d) 0.11 pg·mL^{-1}, (e) 1.1 pg·mL^{-1}, (f) 11 pg·mL^{-1}, (g) 0.11 ng·mL^{-1}, (h) 1.1 ng·mL^{-1}, and (i) 11 ng·mL^{-1}. (D) Calibration plot of the ECL intensity vs. the logarithm of cTnI concentration. Reproduced with permission of Ref. [66], copyright 2018 American Chemical Society.

Table 2. MOFs as carriers for ECL immunoassays.

Labeled composition	Surface	Target	Linear range	LOD	Ref.
Fe(III)-MIL-88 B-NH_2@ZnSeQDs	electropolymerized dopamine MIP	SCCA	$0.1 \times 10^{-3} - 100$ ng·mL^{-1}	31 fg·mL^{-1}	[67]
SnS_2QDs@MIL-101(Cr)	CuS/2D high porous carbon	Carbohydrate antigen 24-2	$0.1 \times 10^{-3} - 100$ U·mL^{-1}	15 μU·mL^{-1}	[68]
Ag^+@UiO-66-NH_2@CdWS	Au/rGO	PSA	$0.1 \times 10^{-3} - 10$ ng·mL^{-1}	38 fg·mL^{-1}	[69]
Ti(IV)-MIL-125	AgNCs-Sem@AuNPs	NT-proBNP	$2.5 \times 10^{-4} - 100$ ng·mL^{-1}	0.11 pg·mL^{-1}	[70]
Fe_3O_4@PDA-Cu_xO	MIL-101(AI):Ru-PEI-Au	Procalcitonin	$5 \times 10^{-4} - 100$ ng·mL^{-1}	0.18 pg·mL^{-1}	[71]
Ru-MOFs	Pd@Au-L-Cys	Apo-A1	$1 \times 10^{-6} - 1.00$ ng·mL^{-1}	1 fg·mL^{-1}	[72]
MMOF@CdSnS	Ag@rGO	AFP	$1 \times 10^{-6} - 100$ ng·mL^{-1}	0.2 fg·mL^{-1}	[73]
Co-MOFs/ABEI	Fe_3O_4@PPy-Au	Aβ42	$1 \times 10^{-5} - 100$ ng·mL^{-1}	3 fg·mL^{-1}	[74]
/	Ce-MOF@g-C_3N_4/Au	NT-proBNP	$5 \times 10^{-3} - 20$ ng·mL^{-1}	3.59 pg·mL^{-1}	[75]
/	MOF-545-Zn@MoS_2QDs	CEA	0.18—1000 ng·mL^{-1}	0.45 pg·mL^{-1}	[76]
/	$Ru(bpy)_3^{2+}$@UiO-66-NH_2	CA15-3	$5 \times 10^{-4} - 500$ U·mL^{-1}	0.17705 μU·mL^{-1}	[77]
/	Ru-MOFs	FABP	$1.5 \times 10^{-4} - 150$ ng·mL^{-1}	2.6 fg·mL^{-1}	[78]

MIP: molecularly imprinted polymer; rGO: reduced graphene oxide; Apo-A1: Apolipoprotein-A1; ABEI: N-(aminobutyl)-N-(ethyl-isoluminol); Aβ42: Amyloid-β protein; FABP: human heart-type fatty-acid-binding protein.

novel strategy for the construction of water-stable MOFs has become a critical direction in the MOF research field. Thirdly, the effective and precise immobilization of antibody or enzyme molecules on specific sites of MOFs remains a challenge. Therefore, developing the methods to control their decorated groups as well as the shape and size may need to be systematically studied to improve the active areas, the functionalization efficiency and accuracy. Finally, MOFs-based electrochemical and ECL immunosensors are usually not inconvenient and suitable for in situ and practical applications, such as rapid on-site disease screening and POC diagnostic. The development of portable devices provides an opportunity to MOFs-based immunosensor for wide applications. We believe that with the development of science and technology, a variety of new MOF nanomaterials with high performance will be synthesized, which will eventually facilitate their industrial implementation, including global health in developing nations, environmental surveillance, and food safety inspection.

Acknowledgements

Thanks for the financial supports from the Natural Sciences and Engineering Research Council of Canada of Canada (NSERC, DG RGPIN-2013-201697 (Z.D.) and RGPIN-2018-06556 (Z.D.)), Canada Foundation of Innovation/Ontario Innovation Trust (CFI/OIT, 9040 (Z.D.)), Premier's Research Excellence Award (PREA, 2003 (Z.D.)), Canada Institute of Photonics Innovation (2005 (Z.D.)), Ontario Photonics Consortium (2002 Z.D.)), National Natural Science Foundation of China (22004034 (X.Q.)), Natural Science Foundation of Hunan Province (China) (2020JJ5226 (X.Q.)) and China Scholarship Council (CSC, 201908430010 (X.Q.)).

References

[1] Karimzadeh Z, Hasanzadeh M, Isildak I, Khalilzadeh B. Multiplex bioassaying of cancer proteins and biomacromolecules: nanotechnological, structural and technical perspectives[J]. Int. J. Biol. Macromol., 2020, 165: 3020−3039.

[2] Tang Z X, Ma Z F. Multiple functional strategies for amplifying sensitivity of amperometric immunoassay for tumor markers: a review[J]. Biosens. Bioelectron., 2017, 98: 100−112.

[3] Shahriyari H A, Nikmanesh Y, Jalali S, Tahery N, Fard A Z, Hatamzadeh N, Zarea K, Cheraghi M, Mohammadi M J. Air pollution and human health risks: mechanisms and clinical manifestations of cardiovascular and respiratory diseases[J]. Toxin Rev., 2022, 41(2): 606−617.

[4] Chiner-Vives E, Cordovilla-Perez R, De la Rosa-Carrillo D, Garcia-Clemente M, Izquierdo-Alonso J L, Otero-Candelera R, Perez-de Llano L, Sellares-Torres J, de Granda-Orive J I. Short and long-term impact of covid-19 infection on previous respiratory diseases[J]. Arch Bronconeumol, 2022, 58: 39−50.

[5] Hunter B, Hindocha S, Lee R W. The role of artificial intelligence in early cancer diagnosis[J]. Cancers, 2022, 14(6): 1524.

[6] Meng H Y, Ruan J J, Yan Z H, Chen Y Q, Liu J S, Li X D, Meng F B. New progress in early diagnosis of atherosclerosis[J]. Int. J. Mol. Sci., 2022, 23(16): 8939.

[7] Fang L, Liao X F, Jia B Y, Shi L C, Kang L Z, Zhou L D, Kong W J. Recent progress in immunosensors for pesticides[J]. Biosens. Bioelectron, 2020, 164: 112255.

[8] Kim J, Park M. Recent progress in electrochemical immunosensors[J]. Biosensors, 2021, 11(10): 360.

[9] Yang Z, Atiyas Y, Shen H, Siedlik M J, Wu J, Beard K, Fonar G, Dolle J P, Smith D H, Eberwine J H, Meaney D F, Issadore D A. Ultrasensitive single extracellular vesicle detection using high throughput droplet digital enzyme-linked immunosorbent assay[J]. Nano Lett, 2022, 22(11): 4315−4324.

[10] Gao Y, Zhou Y Z, Chandrawati R. Metal and metal oxide nanoparticles to enhance the performance of enzyme-linked immunosorbent assay (ELISA)[J]. ACS Appl. Nano Mater., 2020, 3(1): 1−21.

[11] Lyu A H, Jin T C, Wang S S, Huang X X, Zeng W H, Yang R, Cui H. Automatic label-free immunoassay with high sensitivity for rapid detection of sars-cov-2 nucleocapsid protein based on chemiluminescent magnetic beads[J]. Sens. Actuator B-Chem., 2021, 349: 130739.

[12] Xu L R, Cao Z Y, Ma R L, Wang Z Z, Qin Q, Liu E Y, Su B. Visualization of latent fingermarks by enhanced chemiluminescence immunoassay and pattern recognition[J]. Anal. Chem., 2019, 91(20): 12859−12865.

[13] Orme M E, Voreck A, Aksouh R, Ramsey-Goldman R, Schreurs M WJ. Systematic review of anti-dsDNA testing for systemic lupus erythematosus: a meta-analysis of the diagnostic test specificity of an anti-dsDNA fluorescence enzyme immunoassay[J]. Autoimmun. Rev., 2021, 20(11): 102943.

[14] Li H F, Wen K, Dong B L, Zhang J, Bai Y C, Liu M G, Li P P, Mujtaba M G, Yu X Z, Yu W B, Ke Y B, Shen J Z, Wang Z H. Novel inner filter effect-based fluorescence immunoassay with gold nanoclusters for bromadiolone detection in human serum[J]. Sens. Actuator B-Chem., 2019, 297: 126787.

[15] Zhang Y, Zhang R, Yang X L, Qi H L, Zhang C X. Recent advances in electrogenerated chemiluminescence biosensing methods for pharmaceuticals[J]. J. Pharm. Anal., 2019, 9(1): 9−19.

[16] Du F X, Chen Y Q, Meng C D, Lou B H, Zhang W, Xu G B. Recent advances in electrochemiluminescence immunoassay based on multiple-signal strategy[J]. Curr. Opin. Electrochem., 2021, 28: 100725.

[17] Tang D, Yang X, Wang B, Ding Y, Xu S, Liu J, Peng Y, Yu X, Su Z, Qin X. One-step electrochemical growth of 2D/3D Zn(ii)-MOF hybrid nanocomposites on an electrode and utilization of a PtNPs@2D MOF nanocatalyst for electrochemical immunoassay[J]. ACS Appl. Mater. Interfaces, 2021, 13(39): 46225−46232.

[18] Feng J J, Chu C S, Ma Z F. Fenton and Fenton-like catalysts for electrochemical immunoassay: a mini review[J]. Electrochem. Commun., 2021, 125: 106970.

[19] Nellaiappan S, Mandali P K, Prabakaran A, Krishnan U M. Electrochemical immunosensors for quantification of procalcitonin: progress and prospects[J]. Chemosensors, 2021, 9(7): 182.

[20] Tang J, Tang D P. Non-enzymatic electrochemical immunoassay using noble metal nanoparticles: a review[J]. Microchim. Acta, 2015, 182(13−14): 2077−2089.

[21] Pan M F, Gu Y, Yun Y G, Li M, Jin X C, Wang S. Nanomaterials for electrochemical immunosensing[J]. Sensors, 2017, 17(5): 1041.
[22] Sanchez A, Villalonga A, Martinez-Garcia G, Parrado C, Villalonga R. Dendrimers as soft nanomaterials for electrochemical immunosensors[J]. Nanomaterials, 2019, 9(12): 1745.
[23] Feng T T, Wang Y, Qiao X W. Recent advances of carbon nanotubes-based electrochemical immunosensors for the detection of protein cancer biomarkers[J]. Electroanalysis, 2017, 29(3): 662−675.
[24] Popov A, Brasiunas B, Kausaite-Minkstimiene A, Ramanaviciene A. Metal nanoparticle and quantum dot tags for signal amplification in electrochemical immunosensors for biomarker detection[J]. Chemosensors, 2021, 9(4): 85.
[25] Yang H L, Xu W T, Zhou Y. Signal amplification in immunoassays by using noble metal nanoparticles: a review [J]. Microchim. Acta, 2019, 186(12): 859.
[26] Liu H, Cheng Y, Chen Y Y, Xiao H B, Sui Y Y, Xie Q J, Liu R S, Yang X P. Dual-signal sandwich-type electrochemical immunoassay of galectin-3 using methylene blue and gold nanoparticles biolabels[J]. J. Electroanal. Chem., 2020, 861: 113952.
[27] Wang X Y, Chen Y, Mei L P, Wang A J, Yuan P X, Feng J J. Confining signal probe in porous PdPtCoNi@Pt-skin nanopolyhedra to construct a sandwich-type electrochemical immmunosensor for ultrasensitive detection of creatine kinase-mb[J]. Sens. Actuator B-Chem., 2020, 315: 128088.
[28] Zhang S, Rong F L, Guo C AP, Duan F H, He L H, Wang M H, Zhang Z H, Kang M M, Du M. Metal-organic frameworks (MOFs) based electrochemical biosensors for early cancer diagnosis in vitro[J]. Coord. Chem. Rev., 2021, 439: 213948.
[29] Ru J, Wang X M, Wang F B, Cui X L, Du X Z, Lu X Q. Uio series of metal-organic frameworks composites as advanced sorbents for the removal of heavy metal ions: synthesis, applications and adsorption mechanism[J]. Ecotox. Environ. Safe., 2021, 208: 111577.
[30] Lv M Z, Zhou W, Tavakoli H, Bautista C, Xia J F, Wang Z H, Li X J. Aptamer-functionalized metal-organic frameworks (MOFs) for biosensing[J]. Biosens. Bioelectron., 2021, 176: 112947.
[31] Xie L S, Skorupskii G, Dincă M. Electrically conductive metal-organic frameworks[J]. Chem. Rev., 2020, 120(16): 8536−8580.
[32] Su Z H, Tang D L, Yang X L, Peng Y, Wang B R, Li X Y, Chen J H, Hu Y, Qin X L. Selective and fast growth of Cds nanocrystals on zinc (ii) metal-organic framework architectures for photoelectrochemical response and electrochemical immunosensor of foot-and-mouth disease virus [J]. Microchem. J., 2022, 174: 107038.
[33] Cheng Y D, Datta S J, Zhou S, Jia J T, Shekhah O, Eddaoudi M. Advances in metal-organic framework-based membranes[J]. Chem. Soc. Rev., 2022, 51: 8300−8350.
[34] Tran V A, Do H H, Le V T, Vasseghian Y, Vo V, Ahn S H, Kim S Y, Lee S W. Metal-organic-framework-derived metals and metal compounds as electrocatalysts for oxygen evolution reaction: a review[J]. Int. J. Hydrogen Energy, 2022, 47(45): 19590−19608.
[35] Shao M Z, Li Y Y, Chen M Y, Liu W D, Sun Y Z, Chu Y Y, Sun Y J, Li X Y, Zhang R Z, Zhang L B. High-efficiency electrogenerated chemiluminescence of novel Zr-based metal-organic frameworks through organic linkers regulation[J]. ChemElectroChem, 2022, 9(19): e202200866.
[36] Rong S Z, Zou L N, Zhu Y, Zhang Z, Liu H F, Zhang Y C, Zhang H, Gao H M, Guan H J, Dong J, Guo Y P, Liu F H, Li X X, Pan H Z, Chang D. 2D/3D material amplification strategy for disposable label-free electrochemical immunosensor based on rGO-TEPA@Cu-MOFs@SiO_2@AgNPs composites for NMP22 detection[J]. Microchem. J., 2021, 168: 106410.
[37] Mehmandoust M, Gumus Z P, Soylak M, Erk N. Electrochemical immunosensor for rapid and highly sensitive detection of SARS-CoV-2 antigen in the nasal sample[J]. Talanta, 2022, 240: 123211.
[38] Li Y, Wang C B, Li Z Z, Wang M H, He L H, Zhang Z H. Zirconium-porphyrin complex as novel nanocarrier for label-free impedimetric biosensing neuron-specific enolase [J]. Sens. Actuator B-Chem., 2020, 314: 128090.
[39] Gu C X, Guo C P, Li Z Z, Wang M H, Zhou N, He L H, Zhang Z H, Du M. Bimetallic ZrHf-based metal-organic framework embedded with carbon dots: ultra-sensitive platform for early diagnosis of HER2 and HER2-overexpressed living cancer cells[J]. Biosens Bioelectron, 2019, 134: 8−15.
[40] Song Y P, Xu M R, Li Z Z, He L N, Hu M Y, He L H, Zhang Z H, Du M. A bimetallic CoNi-based metal-organic framework as efficient platform for label-free impedimetric sensing toward hazardous substances[J]. Sens. Actuator B-Chem., 2020, 311: 127927.
[41] Bajpai V K, Haldorai Y, Khan I, Sonwal S, Singh M P, Yadav S, Paray B A, Jan B L, Kang S M, Huh Y S, Han Y K, Shukla S. Au@Zr-based metal-organic framework composite as an immunosensing platform for determination of hepatitis b virus surface antigen[J]. Microchim. Acta, 2021, 188(11): 365.
[42] Li L Z, Liu X, Su B C, Zhang H Y, Li R, Liu Z L, Chen Q, Huang T Z, Cao H M. An innovative electrochemical immunosensor based on nanobody heptamer and AuNPs@ZIF-8 nanocomposites as support for the detection of alpha fetoprotein in serum[J]. Microchem. J., 2022, 179: 107463.
[43] Liu H, Chen Y Y, Cheng Y, Xie Q J, Liu R S, Yang X P. Immunosensing of NT-proBNP via Cu^{2+}-based MOFs biolabeling and *in situ* microliter-droplet anodic stripping voltammetry[J]. Electroanalysis, 2020, 32(8): 1754−1762.
[44] Liu J B, Shang Y H, Zhu Q Y, Zhang X X, Zheng J B. A voltammetric immunoassay for the carcinoembryonic antigen using silver(i)-terephthalate metal-organic frameworks containing gold nanoparticles as a signal probe[J]. Mikrochim. Acta, 2019, 186(8): 509.
[45] Liu T Z, Hu R, Zhang X, Zhang K L, Liu Y, Zhang X B, Bai R Y, Li D, Yang Y H. Metal-organic framework nanomaterials as novel signal probes for electron transfer mediated ultrasensitive electrochemical immunoassay[J]. Anal. Chem., 2016, 88(24): 12516−12523.
[46] Bai R Y, Zhang K L, Li D L, Zhang X, Liu T Z, Liu Y, Hu R, Yang Y H. Preparation of carcinoembryonic antigen immunosensor based on Au nanoparticles loaded-metal-organic frameworks[J]. Chinese J. Anal. Chem., 2017, 45(1): 48−55.
[47] Liu X B, Yue T, Qi K, Qiu Y B, Guo X P. Porous graphene based electrochemical immunosensor using $Cu_3(BTC)_2$ metal-organic framework as nonenzymatic label[J]. Talanta, 2020, 217: 121042.
[48] Zhang C, Zhang D S, Ma Z F, Han H L. Cascade catalysis-initiated radical polymerization amplified impedimetric immunosensor for ultrasensitive detection of carbohydrate antigen 15-3[J]. Biosens. Bioelectron., 2019, 137: 1−7.
[49] Feng J J, Wang H Q, Ma Z F. Ultrasensitive amperometric immunosensor for the prostate specific antigen by exploiting a fenton reaction induced by a metal-organic framework nanocomposite of type Au/Fe-MOF with peroxidase mimicking activity[J]. Microchim. Acta, 2020, 187(1): 95.
[50] Dong H, Liu S H, Liu Q, Li Y Y, Li Y Y, Zhao Z D. A dual-signal output electrochemical immunosensor based on Au-MoS_2/MOF catalytic cycle amplification strategy for neuron-specific enolase ultrasensitive detection[J]. Biosens. Bioelectron., 2022, 195: 113648.

[51] Zhang K L, Dai K, Bai R Y, Ma Y C, Deng Y, Li D L, Zhang X, Hu R, Yang Y H. A competitive microcystin-LR immunosensor based on Au NPs@metal-organic framework (MIL-101)[J]. Chinese Chem. Lett., 2019, 30(3): 664−667.

[52] Parvin S, Hashemi P, Afkhami A, Ghanei M, Bagheri H. Simultaneous determination of BoNT/A and/E using an electrochemical sandwich immunoassay based on the nanomagnetic immunosensing platform[J]. Chemosphere, 2022, 298: 134358.

[53] Liu C, Dong J, Ning S, Hou J, Waterhouse G IN, Cheng Z, Ai S. An electrochemical immunosensor based on an etched zeolitic imidazolate framework for detection of avian leukosis virus subgroup J[J]. Microchim. Acta, 2018, 185(9): 423.

[54] Feng J J, Liang X Y, Ma Z F. New immunoprobe: dual-labeling ZIF-8 embellished with multifunctional bovine serum albumin lamella for electrochemical immunoassay of tumor marker[J]. Biosens. Bioelectron., 2021, 175: 112853.

[55] Feng J J, Yao T, Chu C S, Ma Z F, Han H L. Proton-responsive annunciator based on i-motif DNA structure modified metal organic frameworks for ameliorative construction of electrochemical immunosensing interface[J]. J. Colloid Interface Sci., 2022, 608(Pt 2): 2050−2057.

[56] Li W J, Ma C Y, Song Y J, Hong C L, Qiao X W, Yin B C. Sensitive detection of carcinoembryonic antigen (CEA) by a sandwich-type electrochemical immunosensor using MOF-Ce@HA/Ag-HRP-Ab2 as a nanoprobe[J]. Nanotechnology, 2020, 31(18): 185605.

[57] Han J, Zhang M F, Chen G J, Zhang Y Q, Wei Q, Zhuo Y, Xie G, Yuan R, Chen S P. Ferrocene covalently confined in porous MOF as signal tag for highly sensitive electrochemical immunoassay of amyloid-beta[J]. J. Mat. Chem. B, 2017, 5(42): 8330−8336.

[58] Liu J B, Shang Y H, Xu J Q, Chen Y, Jia Y R, Zheng J B. A novel electrochemical immunosensor for carcinoembryonic antigen based on Cu-MOFs-TB/polydopamine nanocarrier[J]. J. Electroanal. Chem., 2020, 877: 114563.

[59] Lu W, Chen Z A, Wei M, Cao X, Sun X. A three-dimensional coni-mof nanosheet array-based immunosensor for sensitive monitoring of human chorionic gonadotropin with core-shell ZnNi-MOF@Nile Blue nanotags[J]. Analyst, 2021, 145(24): 8097−8103.

[60] Zhang P, Huang H, Wang N, Li H J, Shen D Z, Ma H Y. Duplex voltammetric immunoassay for the cancer biomarkers carcinoembryonic antigen and alpha-fetoprotein by using metal-organic framework probes and a glassy carbon electrode modified with thiolated polyaniline nanofibers[J]. Microchim. Acta, 2017, 184(10): 4037−4045.

[61] Zhao G H, Dong X, Du Y, Zhang N, Bai G Z, Wu D, Ma H M, Wang Y G, Cao W, Wei Q. Enhancing electrochemiluminescence efficiency through introducing atomically dispersed ruthenium in nickel-based metal-organic frameworks[J]. Anal. Chem., 2022, 94(29): 10557−10566.

[62] Wang Y G, Zhao G H, Chi H, Yang S H, Niu Q F, Wu D, Cao W, Li T D, Ma H M, Wei Q. Self-luminescent lanthanide metal-organic frameworks as signal probes in electrochemiluminescence immunoassay[J]. J. Am. Chem. Soc., 2021, 143(1): 504−512.

[63] Wang C, Li Z H, Ju H X. Copper-doped terbium luminescent metal organic framework as an emitter and a co-reaction promoter for amplified electrochemiluminescence immunoassay[J]. Anal. Chem., 2021, 93(44): 14878−14884.

[64] Song X Z, Zhao L, Zhang N, Liu L, Ren X, Ma H M, Luo C N, Li Y Y, Wei Q. Zinc-based metal-organic framework with MLCT properties as an efficient electrochemiluminescence probe for trace detection of trenbolone [J]. Anal. Chem., 2022, 94(40): 14054−14060.

[65] Li J S, Jia H Y, Ren X, Li Y Y, Liu L, Feng R Q, Ma H M, Wei Q. Dumbbell plate-shaped aiegen-based luminescent mof with high quantum yield as self-enhanced ECL tags: mechanism insights and biosensing application[J]. Small, 2022, 18(13): e2106567.

[66] Yang X, Yu Y Q, Peng L Z, Lei Y M, Chai Y Q, Yuan R, Zhuo Y. Strong electrochemiluminescence from MOF accelerator enriched quantum dots for enhanced sensing of trace ctni[J]. Anal. Chem., 2018, 90(6): 3995−4002.

[67] Mo G C, Qin D M, Jiang X H, Zheng X F, Mo W M, Deng B Y. A sensitive electrochemiluminescence biosensor based on metal-organic framework and imprinted polymer for squamous cell carcinoma antigen detection[J]. Sens. Actuator B-Chem., 2020, 310: 127852.

[68] Shen C Q, Li Y, Li Y M, Wang S J, Li Y Y, Tang F, Wang P, Liu H, Li Y Y, Liu Q. A double reaction system induced electrochemiluminescence enhancement based on SnS_2 QDs@MIL-101 for ultrasensitive detection of CA242[J]. Talanta, 2022, 247: 123575.

[69] Fang Q C, Lin Z H, Lu F S, Chen Y W, Huang X C, Gao W H. A sensitive electrochemiluminescence immunosensor for the detection of PSA based on CdWS nanocrystals and Ag^{+}@UIO-66-NH_2 as a novel coreaction accelerator[J]. Microchim. Acta, 2019, 302: 207−215.

[70] Dong X, Zhao G H, Li X, Miao J C, Fang J L, Wei Q, Cao W. Electrochemiluminescence immunoassay for the N-terminal pro-B-type natriuretic peptide based on resonance energy transfer between a self-enhanced luminophore composed of silver nanocubes on gold nanoparticles and a metal-organic framework of type MIL-125[J]. Microchim. Acta, 2019, 186(12): 811.

[71] Wu H Y, Li Z Y, Wang Y, Li X, Zhu W H. Inhibition effect of CTAB on electrodeposition of Cu in micro via: experimental and md simulation investigations[J]. J. Electrochem. Soc., 2019, 166(15): D816−D825.

[72] Qi J L, Zhang X L, Zhang Q Y, Xue Y, Meng F, Liu Y H, Yang G J. Ultrasensitive "signal-on" sandwich electrochemiluminescence immunosensor based on Pd@Au-L-cysteine enabled multiple-amplification strategy for apolipoprotein-A1 detection[J]. Microchem. J., 2022, 178: 107409.

[73] Ding Y P, Zhang X, Peng J J, Zheng D L, Zhang X S, Song Y B, Chen Y W, Gao W H. Ultra-sensitive electrochemiluminescence platform based on magnetic metal-organic framework for the highly efficient enrichment[J]. Sens. Actuator B-Chem., 2020, 324: 128700.

[74] Wang F L, Zhang Q L, Zhou K, Le Y P, Liu W, Wang Y, Wang F. Effect of cetyl-trimethyl-ammonium-bromide (CTAB) and bis (3-sulfopropyl) disulfide (SPS) on the through-silicon-via (TSV) copper filling[J]. Microelectron. Eng. 2019: 217.

[75] Li L, Zhao Y H, Li X J, Ma H M, Wei Q. Label-free electrochemiluminescence immunosensor based on Ce-MOF@g-C_3N_4/Au nanocomposite for detection of n-terminal pro-B-type natriuretic peptide[J]. J. Electroanal. Chem., 2019, 847: 113222.

[76] Xin W L, Jiang L F, Zong L P, Zeng H B, Shu G F, Marks R, Zhang X J, Shan D. MoS_2 quantum dots-combined zirconium-metalloporphyrin frameworks: synergistic effect on electron transfer and application for bioassay[J]. Sens. Actuator B-Chem., 2018, 273: 566−573.

[77] Xiong X, Zhang Y, Wang Y F, Sha H F, Jia N Q. One-step electrochemiluminescence immunoassay for breast cancer biomarker CA 15-3 based on $Ru(bpy)_6^{2+}$-coated UIO-66-NH_2 metal-organic framework[J]. Sens. Actuator B-Chem., 2019, 297: 126812.

[78] Qin X L, Zhang X H, Wang M H, Dong Y F, Liu J J, Zhu Z W, Li M X, Yang D, Shao Y H. Fabrication of tris(-bipyridine)ruthenium(ii)-functionalized metal-organic framework thin films by electrochemically assisted self-

assembly technique for electrochemiluminescent immunoassay[J]. Anal. Chem., 2018, 90(19): 11622−11628.
[79] Zhao G H, Wang Y G, Li X J, Dong X, Wang H, Du B, Cao W, Wei Q. Quenching electrochemiluminescence immunosensor based on resonance energy transfer between ruthenium (ii) complex incorporated in the UiO-67 metal-organic framework and gold nanoparticles for insulin detection[J]. ACS Appl. Mater. Interfaces, 2018, 10(27): 22932−22938.
[80] Qin X L, Dong Y F, Wang M H, Zhu Z W, Li M X, Yang D, Shao Y H. *In situ* growing triethanolamine-functionalized metal-organic frameworks on two-dimensional carbon nanosheets for electrochemiluminescent immunoassay[J]. ACS Sens., 2019, 4(9): 2351−2357.

金属有机框架材料在电化学/电化学发光免疫分析中的应用

覃晓丽[a,b,*]，詹子颖[b]，Sara Jahanghiri[b]，Kenneth Chu[b]，张丛洋[b]，丁志峰[b,*]
[a]湖南农业大学化学与材料科学学院，湖南 长沙 410128，中国
[b]Department of Chemistry, Western University, London, Ontario N6A 5B7, Canada

摘要

设计和研制具有超灵敏、高精度、选择性好的免疫传感器对于疾病的早期诊断和筛查以及疾病治疗过程的监测具有十分重要的意义。其中，电化学免疫分析法和电化学发光（ECL）免疫分析法，由于具有稳定性好、灵敏度高、线性范围宽、可控性好等优点而备受关注，已成为当前的研究热点之一。金属有机框架（MOFs）作为一类新型的多孔晶体材料，由于其具有比表面积大、化学稳定性好、孔径和纳米级骨架结构可调节等优点，在电化学和ECL免疫传感器的制备中得到了广泛的应用。MOFs 不仅可以作为固定生物识别分子的敏感平台，还可以用于富集痕量分析物和信号分子来放大分析信号，提高电化学或 ECL 免疫分析的灵敏度。目前，科研人员已合成各种各样具有不同性能和形貌的 MOFs 纳米材料，并用于开发高性能的电化学免疫传感器和 ECL 免疫传感器。本文综述了不同类型的基于 MOFs 纳米材料的电化学/ECL 免疫传感器的制备及其在免疫分析中的检测应用。研究表明，MOFs 不仅可以作为电极表面修饰的基底、信号探针（包括电活性标记分子和电化学发光发光标记探针）、催化活性标记物，还可以作为负载各种生物分子、纳米材料的载体，最终可用于灵敏的电化学和 ECL 检测。此外，本综述还讨论了未来发展功能化 MOFs 纳米材料的挑战和机遇，并为未来设计和制造基于 MOFs 的高性能免疫传感器提出了一些指导性意见。

关键词：金属有机框架；电化学免疫传感器；电化学发光法免疫传感器；免疫分析